Lactate transporters in the rat barrel cortex sustain whisker-dependent BOLD fMRI signal and behavioral performance

Hélène Roumes[a,1], Charlotte Jollé[b,1], Jordy Blanc[a], Imad Benkhaled[a,c], Carolina Piletti Chatain[d], Philippe Massot[a], Gérard Raffard[a], Véronique Bouchaud[a], Marc Biran[a], Catherine Pythoud[e], Nicole Déglon[e], Eduardo R. Zimmer[f], Luc Pellerin[b,g,1], and Anne-Karine Bouzier-Sore[a,1,2]

[a]Centre de Résonance Magnétique des Systèmes Biologiques, UMR 5536, CNRS, Université deBordeaux F-33076 Bordeaux, France; [b]Department of Physiology, Université de Lausanne, Lausanne 1005, Switzerland; [c]I3M, Common Laboratory CNRS-Siemens, University of Poitiers and Poitiers University Hospital F-86073 Poitiers, France; [d]Department of Biochemistry, Universidad Federal do Rio Grande do Sul 90040-060 Porto Alegre, Brazil; [e]Laboratory of Cellular and Molecular Neurotherapies, Neuroscience Research Center, Department of Clinical Neurosciences, Lausanne University Hospital, Université de Lausanne 1015 Lausanne, Switzerland; [f]Department of Pharmacology, Graduate Program in Biological Sciences: Biochemistry and Pharmacology and Therapeutics, Universidad Federal do Rio Grande do Sul 90040-060 Porto Alegre, Brazil; and [g]Ischémie Reperfusion en Transplantation d'Organes Mécanismes et Innovations Thérapeutiques, INSERM U1082, Université de Poitiers and Poitiers University Hospital F-86021 Poitiers, France

Edited by Marcus E. Raichle, Washington University in St. Louis, St. Louis, MO, and approved October 12, 2021 (received for review July 7, 2021)

Lactate is an efficient neuronal energy source, even in presence of glucose. However, the importance of lactate shuttling between astrocytes and neurons for brain activation and function remains to be established. For this purpose, metabolic and hemodynamic responses to sensory stimulation have been measured by functional magnetic resonance spectroscopy and blood oxygen level-dependent (BOLD) fMRI after down-regulation of either neuronal MCT2 or astroglial MCT4 in the rat barrel cortex. Results show that the lactate rise in the barrel cortex upon whisker stimulation is abolished when either transporter is down-regulated. Under the same paradigm, the BOLD response is prevented in all MCT2 down-regulated rats, while about half of the MCT4 down-regulated rats exhibited a loss of the BOLD response. Interestingly, MCT4 down-regulated animals showing no BOLD response were rescued by peripheral lactate infusion, while this treatment had no effect on MCT2 down-regulated rats. When animals were tested in a novel object recognition task, MCT2 down-regulated animals were impaired in the textured but not in the visual version of the task. For MCT4 down-regulated animals, while all animal succeeded in the visual task, half of them exhibited a deficit in the textured task, a similar segregation into two groups as observed for BOLD experiments. Our data demonstrate that lactate shuttling between astrocytes and neurons is essential to give rise to both neurometabolic and neurovascular couplings, which form the basis for the detection of brain activation by functional brain imaging techniques. Moreover, our results establish that this metabolic cooperation is required to sustain behavioral performance based on cortical activation.

brain metabolism | monocarboxylate transporter | fMRI | MRS | learning and memory

In the past 25 y, a major revolution in the field of brain energy metabolism has occurred. While it was believed classically that glucose is the sole valuable energy substrate for neurons, it is now admitted that under certain circumstances, alternative substrates can serve as fuels and replace glucose, at least partially, even in the adult brain. This is the case for lactate. Indeed, it was shown that lactate provided from the periphery through the blood circulation is efficiently used by the brain in animals (1) and humans (2–4). In addition to peripheral supply, the brain itself has the capacity to internally produce lactate from blood-borne glucose. This process of activity-dependent lactate transfer is named the astrocyte–neuron lactate shuttle (ANLS) (5) and has received a large support in the literature based on in vitro (6, 7), ex vivo (1), and in vivo experiments (8–11). It was also shown that lactate supply by glial cells to neurons is a fundamental process that has been conserved during evolution, as it was found to be present in invertebrates as well (e.g., flies) (12, 13). Nevertheless, some recent studies have provided evidence that direct glucose utilization by neurons also takes place during activation (14, 15). It might be essential for some aspects of neurotransmission (16) or when metabolized via the pentose phosphate pathway to regenerate glutathione and ensure antioxidant protection (17). These observations call for further in vivo investigations to assess the contribution of these energy-supply modes to sustain brain activities, ranging from metabolic and hemodynamic responses associated with brain activation to behavioral performances.

It has been well documented that activation of a brain region (e.g., hippocampus or cortex) leads to a transient increase in lactate concentration within the activated area in rodents (18–20) and in humans (21, 22). Such an observation might reflect a transient mismatch between lactate production attributed to astrocytes and utilization/disposal by other brain cells, although the importance of each remains to be confirmed in vivo. The capacity to release or utilize lactate is determined by the expression of specific transporters, named monocarboxylate transporters (MCTs).

Significance

For decades, it was claimed that glucose was the sole and sufficient energy substrate to sustain neuronal activity and brain function. Our results challenge this view by demonstrating that despite glucose availability, lactate shuttling from astrocytes to neurons via monocarboxylate transporters is necessary to give rise to the blood oxygen level-dependent signal (used as a surrogate marker for activation) in the rat cerebral cortex following whisker stimulation. Moreover, lactate shuttling turned out to be also essential for sustaining behavioral performance associated with activation of the rat barrel cortex. These findings call for a reappraisal of neuroenergetics and the role of astrocytes in determining brain activation and function.

Author contributions: L.P. and A.-K.B.-S. designed research; H.R., C.J., J.B., C.P.C., V.B., M.B., and A.-K.B.-S. performed research; P.M., G.R., C.P., and N.D. contributed new reagents/analytic tools; H.R., C.J., J.B., I.B., E.R.Z., L.P., and A.-K.B.-S. analyzed data; and H.R., C.J., E.R.Z., L.P., and A.-K.B.-S. wrote the paper.

The authors declare no competing interest.

This article is a PNAS Direct Submission.

[1]H.R., C.J., L.P., and A.-K.B.-S. contributed equally to this work.

[2]To whom correspondence may be addressed. Email: akb@rmsb.u-bordeaux.fr.

Published November 15, 2021.

Three members of this family have been identified in the central nervous system (23): MCT2 is the predominant neuronal lactate transporter (24); MCT4 expression is prominent on astrocytes (25); while MCT1 expression is more ubiquitous with strong expression on endothelial cells of blood vessels as well as on glial cells (26). Previously, it was shown that reducing MCT2 expression (which allows neuronal lactate uptake) interfered with blood oxygen level-dependent (BOLD) fMRI signal, which depends on local, activity-dependent change in blood flow and is used as a surrogate marker for neuronal activity to perform functional brain imaging (20). Recently, new viral vector tools have been developed that allow the down-regulation of either MCT2 or MCT4 expression in a cell-specific manner in vivo (27). In the present study, we took advantage of this approach to determine the importance of both transporters—and by extension, of lactate shuttling between astrocytes and neurons—in both metabolic and hemodynamic responses, as well as in behavioral performances associated with activation of the whisker-to-barrel system in rats.

Results

Cortical Lactate Accumulation Caused by Whisker Stimulation Is Prevented by Either Neuronal MCT2 or Astroglial MCT4 Down-Regulation. The impact of downregulating either the neuronal MCT2 or the astroglial MCT4 transporter in the rat barrel cortex (S1BF area) on the metabolic response to whisker stimulation was evaluated by functional magnetic resonance spectroscopy (fMRS) in vivo. Whiskers were stimulated directly into the magnet, using an MRI-compatible air-puff system. The paradigm was composed of a succession of a 20-s activation period (8 Hz) followed by a 10-s rest to avoid neuronal desensitization (Fig. 1*A*). In vivo ^{1}H-MRS was acquired in a 2 × 2.5 × 3-mm voxel located in the left barrel cortex (Fig. 1*B*). A first acquisition was performed at rest (Fig. 1*B*, blue spectra). Then, right whiskers were stimulated and a second acquisition was recorded (Fig. 1*B*, red spectra). fMRS was performed in rats treated with a control adeno-associated vector (AAV) expressing a nonspecific sequence (control, Ctrl; white), or rats injected with vectors inducing the knockdown of MCT2 (MCT2-KD) (Fig. 1, purple) or MCT4 (MCT4-KD) (Fig. 1, orange). The signal from protons of the methyl group of lactate is located at 1.32 ppm. The subtraction of the two spectra (activated – rest) is represented in black. While an increase in lactate content in the barrel cortex can be observed in Ctrl rats, this increase was abolished both in MCT2- and MCT4-KD rats. Quantification of metabolite contents was performed using LCModel and the ratio [lactate content during whisker activation] over [lactate content at rest] is presented in Fig. 1*C*. This ratio was 1.25 ± 0.05 in control rats, a statistically significant increase of 25% in lactate content during whisker activation, while this ratio was 1.03 ± 0.04 and 1.04 ± 0.04, in MCT2- and MCT4-KD rats, respectively, which confirms the absence of lactate increase in these animals. No statistical difference was found between Ctrl (1.25 ± 0.05, $n = 23$) and uninjected rats (1.30 ± 0.09, $n = 16$; $P = 0.0833$).

To determine the origin of the lactate that accumulates during whisker activation, [1-^{13}C]glucose was infused in awake rats. During the 1-h infusion, right whiskers were stimulated (same paradigm as the one used for in vivo MRS) (Fig. 2*A*). At the end of the infusion, both right (at rest) and left (activated) barrel cortices were removed (Fig. 2*A*) and ex vivo MRS was performed on the perchloric acid extracts using a proton-observed carbon-edited (POCE) sequence. This sequence enabled the quantification of some metabolite specific enrichments, which represent the percentage of ^{13}C incorporated into a carbon position from the ^{13}C-labeled substrate that was infused (Fig. 2*E*). For Ctrl rats, results indicate an increase in the specific enrichment of lactate carbon 3 (C3) between rest (8.7%) and activated (11.3%) barrel cortices (+30%), while the one of glutamine C4 decreased (from 11.1 to 7.3%). [3-^{13}C]pyruvate, produced from [1-^{13}C]glucose at the end of glycolysis, can either be converted into [3-^{13}C]lactate or go into the TCA cycle, from which [4-^{13}C]glutamine will be labeled (for a detailed fate of [1-^{13}C]glucose, see ref. 28). The increase in [3-^{13}C]lactate-specific enrichment, together with a parallel decrease in [3-^{13}C]glutamine-specific enrichment in Ctrl rats during whisker stimulation, reflects a relative increase in glycolysis compared to the TCA cycle during activation, which was not observed in MCT-KD rats. Indeed, for both MCT2- and MCT4-KD rats, no statistical difference between rest and activated barrel cortices was found. Comparison of lactate C3-specific enrichments between the right barrel cortex (resting hemisphere) and the left one (activated hemisphere) for each individual rat is shown in Fig. 2*B* (Ctrl), Fig. 2*C* (MCT2) and Fig. 2*D* (MCT4). For Ctrl rats, it can be clearly seen that whisker stimulation led to an increase in the incorporation of ^{13}C in lactate, indicating that more [3-^{13}C]lactate was produced from the infused precursor, [1-^{13}C]glucose, in the activated brain area. This was not observed for MCT2-KD rats. Concerning MCT4-KD rats, two animals showed a clear increase in the specific enrichment of lactate C3 between the right and the left hemispheres, whereas an obvious decrease was measured in three animals and slightly the same values were observed in seven MCT4-KD rats.

Cortical BOLD Signal Triggered by Whisker Activation Requires MCT2-Dependent Neuronal Lactate Shuttling Provided at Least in Part by Astrocytes via MCT4. To understand why no metabolic response (observed as lactate accumulation) was detected in the barrel cortex during whisker stimulation in MCT2- and MCT4-KD rats, BOLD fMRI was performed. The 5-min paradigm used during whisker stimulation was the same as the one used during in vivo MRS and is presented Fig. 3*A*. For Ctrl rats, a positive BOLD signal was recorded in 95% of the rats (Fig. 3*B*) ($n = 22$). When the neuronal monocarboxylate transporter (MCT2) was down-regulated, a positive BOLD fMRI signal was observed in only 12% of the animals. Moreover, in the four BOLD^{+} MCT2-KD rats, brain activation level was much lower than in controls as shown in Fig. 3*C* (only signals in BOLD-responding animals were quantified). In the MCT4-KD group, 53% of the rats (9 of 17 animals; positively responding rats) had a positive BOLD signal. For these MCT4-BOLD–responding animals, no statistical difference was found in BOLD signal intensity compared to Ctrl rats. In contrast, 47% of the MCT4-KD rats (8 of 17 animals; nonresponding rats) had no BOLD fMRI signal.

Rescue experiments were performed in Ctrl, MCT2-KD, and MCT4-KD rats (Fig. 3*E*). For those, a first BOLD fMRI was acquired, then lactate was infused via the tail vein to the animal, and a second BOLD fMRI was recorded 10 min after starting lactate infusion (this time point was determined such as the lactate concentration in the barrel cortex, measured by in vivo MRS, was the highest with an increase of ∼50%) (Fig. 3*D*). When sodium lactate was infused during whisker activation, no difference was observed in BOLD fMRI signals measured before or during lactate infusion, neither in Ctrl rats (similar positive BOLD fMRI signal before or during lactate infusion) nor in MCT2-KD rats (no BOLD signal, before or during lactate infusion). Interestingly, data for MCT4-KD animals can be clearly divided into two subgroups; responding animals (during the first BOLD fMRI experiment, called MCT4 Resp) and nonresponding animals (MCT4 Non-resp). An increase in the BOLD fMRI signal was observed between the first (without lactate infusion) and the second (during lactate infusion) BOLD fMRI acquisitions in initially nonresponding animals only (5 of 10 animals). Increases in signal between the first and the second BOLD fMRI acquisitions are shown in Fig. 3*F*.

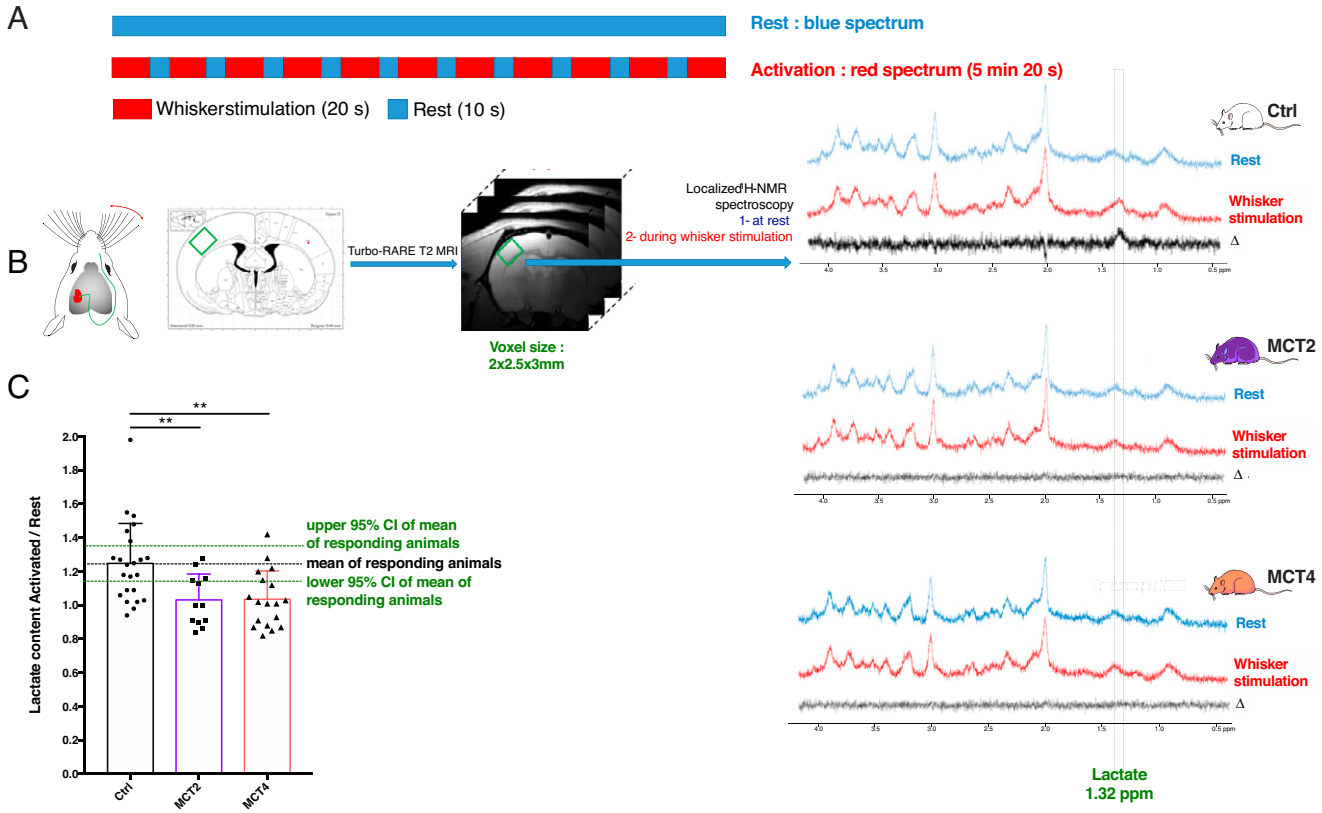

Fig. 1. In vivo fMRS upon whisker stimulation in rats with cell-specific MCT2 or MCT4 down-regulation in the barrel cortex. (*A*) Whisker stimulation paradigm (activation: 20 s, 8 Hz; rest: 10 s to avoid neuronal desensitization, during the entire MRS acquisition for the activation condition: 128 scans, 5 min 20 s). (*B*) The right whisker stimulation leads to the activation of the barrel cortex (also called S1BF) in the left somatosensory cortex. Voxel location for MRS is determined by comparison of T2-weighted images and rat atlas maps. Typical spectra acquired at rest (blue) and during whisker stimulation (red) for Ctrl, MCT2- and MCT4-KD rats. The difference between the red and the blue spectra is shown in the black spectra. The green rectangle indicates the chemical shift of the protons from the methyl group of lactate (protons linked to lactate carbon 3) at 1.32 ppm. (*C*) Ratio of lactate contents during the whisker stimulation and the resting state. Ctrl, $n = 23$; MCT2, $n = 12$; MCT4, $n = 18$. $^{**}P < 0.004$; one-way ANOVA followed by a Fisher's LSD test.

Learning Involving the Whisker-to-Barrel System Requires Intact Neuronal MCT2 Expression and at Least in Part Intact Astroglial MCT4 Expression in the Barrel Cortex. To determine if the absence of the BOLD signal in the barrel cortex upon whisker activation can lead to a loss-of-function, we developed a textured novel object recognition (tNOR) task to specifically probe a barrel cortex-dependent behavior. This task was designed to test the impact of MCT KD in the barrel cortex on behavioral performance and was based on two already published protocols (29, 30). Some modifications were set up to avoid any texture recognition with the forepaws and to differentiate whisker-dependent sensory experience from whisker-independent experience (the protocol is presented in Fig. 4*A* and objects are displayed in Fig. 4*B*, *Upper*). As control, we used a classic visual novel object recognition task (vNOR) (objects are presented in Fig. 4*B*, *Lower*). The sensitivity and specificity of the test was controlled using an *N*-methyl-D-aspartate (NMDA) injection in the barrel cortex to produce a localized excitotoxic lesion (31) and thus interfere with behavioral performance related to texture but not to visual information processing (Fig. 4 *C* and *D*).

To analyze the impact of neuronal MCT2 down-regulation in the barrel cortex, animals were submitted to the entire NOR protocol (Fig. 4*E*). Unlike Ctrl rats, MCT2-KD animals were unable to discriminate between the two textures in the tNOR task, reflecting a dysfunction of the barrel cortex. Indeed, this impaired processing of somatosensory information prevented them from learning the task. However, in the vNOR task, their learning capacity was intact as they performed like Ctrl rats. Because of the striking visual difference between the two objects, an additional processing of somatosensory information (via whisking activity) was not necessary for recognition of the objects. Thus, the vNOR task can be considered to be barrel cortex-independent, most likely relying primarily on visual information processing. The impact of downregulating the astrocytic lactate transporter MCT4 was also explored using the NOR protocol (Fig. 4*F*). Ctrl and MCT4-KD rats were both able to discriminate the objects during the vNOR task, while Ctrl rats also succeeded in the tNOR task. In contrast, two distinct behaviors were observed for MCT4-KD rats in the tNOR task (Fig. 4*G*). As already observed during BOLD fMRI experiments, MCT4-KD rats can be divided into two subgroups: a first subgroup was clearly unable to discriminate the textured objects (discrimination index, 0.49 ± 0.04; 10/18 animals), while the second subgroup was able to discriminate the two different textured objects (discrimination index, 0.69 ± 0.06; 8/18 MCT4-KD rats).

Discussion

Three decades ago, a rise in lactate levels was observed for the first time in the visual cortex of humans by in vivo MRS during a photic stimulation (21, 22). At that time, this observation was attributed to a transient increase in glycolysis over respiration during brain activation. Recently, we developed a technique to perform similar in vivo MRS during brain activation in the rat barrel cortex (32). Using this technique, our aim was to follow lactate fluctuations linked to brain activity (obtained by whisker

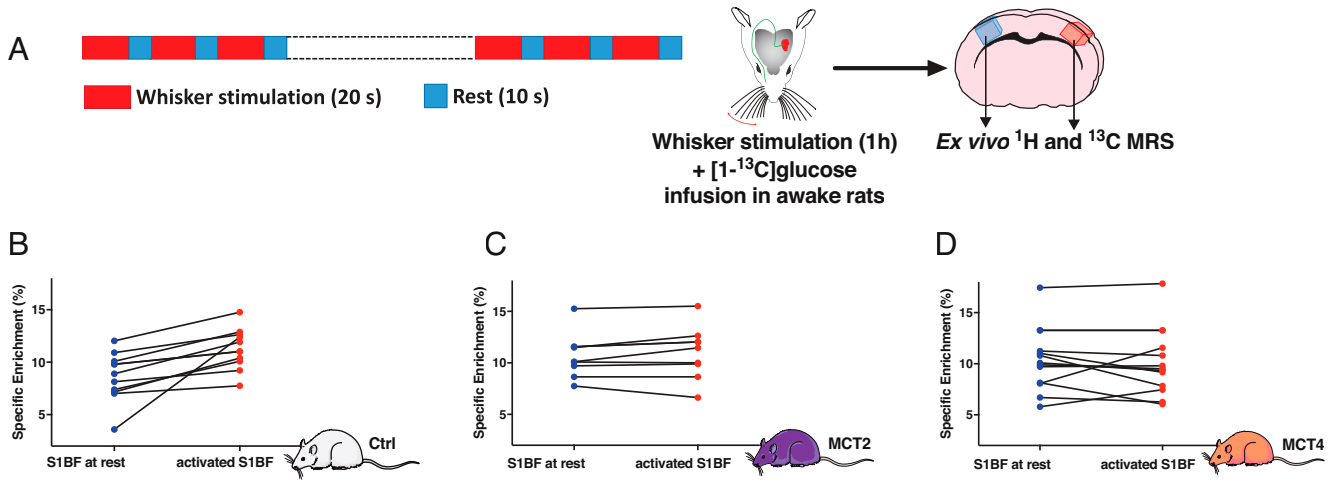

E

	Ctrl		MCT2		MCT4	
	S1BF -	S1BF +	S1BF -	S1BF +	S1BF -	S1BF +
Lac C3	**8.6 ± 0.7**	**11.3 ± 0.6****	**10.7 ± 0.7**	**11.0 ± 0.8**	**10.4 ± 0.8**	**10.2 ± 0.9**
Ala C3	12.5 ± 0.7	14.0 ± 0.9	13.6 ± 0.6	13.9 ± 1.1	13.0 ± 0.7	13.3 ± 0.7
GABA C2	13.3 ± 0.7	13.8 ± 0.9	13.5 ± 0.7	14.4 ± 1.2	13.8 ± 0.7	12.8 ± 0.5
Glu C4	13.2 ± 1.1	12.9 ± 1.1	14.3 ± 0.9	13.2 ± 1.5	12.4 ± 1.0	13.4 ± 0.8
Gln C4	**11.1 ± 1.2**	**7.3 ± 1.1***	**7.6 ± 1.2**	**8.6 ± 1.5**	**8.8 ± 1.6**	**10.3 ± 1.1**
Asp C3	9.7 ± 1.1	11.7 ± 1.3	10.2 ± 1.0	12.1 ± 0.9	9.1 ± 0.8	10.3 ± 0.9

Fig. 2. Comparison of lactate C3 ^{13}C-specific enrichments (%) between the resting hemisphere (right S1BF, blue) and the activated hemisphere (left S1BF, red). (*A*) Paradigm used for whisker stimulation (activation: 20 s, 8 Hz; rest: 10 s, during the entire [1-^{13}C]glucose infusion protocol: 1 h). (*B*) Comparison of [3-^{13}C]lactate specific enrichment (%) for each animal between the resting and activated S1BF in Ctrl rats, $n = 10$, $P = 0.004$, between right and left hemispheres, paired *t* test. (*C*) Comparison of [3-^{13}C]lactate specific enrichment (%) for each animal between the resting and activated S1BF in MCT2-KD rats, $n = 8$. (*D*) Comparison of [3-^{13}C]lactate specific enrichment (%) for each animal between the resting and activated S1BF in MCT4-KD rats, $n = 12$. (*E*) ^{13}C-specific enrichment values for some metabolites (%). [1-^{13}C]glucose was infused in the tail vein and the ^{13}C incorporation in some metabolites was measured from POCE spectra of perchloric acid extracts of resting and activated S1BF in Ctrl, MCT2-, and MCT4-KD rats. Ala C3: carbon 3 of alanine; Asp C3: carbon 3 of aspartate; GABA C2: carbon 2 of γ-aminobutyrate; Gln C4: carbon 4 of glutamine; Glu C4: carbon 4 of glutamate; Lac C3: carbon 3 of lactate.*$P < 0.05$; **$P = 0.017$; ordinary one-way ANOVA, followed by Fisher's LSD test. Ctrl, $n = 10$; MCT2, $n = 8$; and MCT4, $n = 12$.

stimulation) in animals in which key partners of the ANLS would be down-regulated. Right whisker stimulation led to an increase in lactate content in the left barrel cortex (also called S1BF) in Ctrl rats (receiving the viral vector but expressing a nonspecific sequence). The same increase in lactate was observed in noninjected rats, indicating that the stereotaxic injection of AAVs has no impact on our observed signal. Considering that brain lactate concentration was around 1 mM (measured in the barrel cortex at rest by in vivo MRS), this 25 to 30% increase would bring lactate concentration in the S1BF area around 1.25 to 1.30 mM. Keeping in mind the huge difference between neuronal activation and in vivo fMRS recording scales (milliseconds vs. minutes), this new lactate concentration may reflect a previously unrecorded steady state, in which the lactate concentration is enhanced, putatively to support high neuronal energy needs during brain activity. This new steady state in lactate concentration in the activated S1BF during whisker stimulation can be explained either by an increase in lactate synthesis during neuronal activity or by a decrease in its consumption. To distinguish between these two hypotheses, we performed ^{13}C-experiments in which [1-^{13}C]glucose was infused in awake animals during right whisker activation. Then, both right and left barrel cortices were analyzed by ex vivo ^{1}H and ^{13}C-NMR spectroscopy. We measured an increase in the specific enrichment of [3-^{13}C] lactate in the activated S1BF in Ctrl rats. This means that neuronal stimulation led to a greater synthesis of lactate (^{13}C-labeled) in the activated zone, the precursor being [1-^{13}C]glucose infused in the blood circulation. This result confirms previous data obtained using ex vivo MRS on control rats (33) and indicates that lactate is produced from blood-circulating glucose within the brain area during neuronal activity, at least in the cortex.

When the neuronal lactate transporter MCT2 was down-regulated in the rat barrel cortex, no lactate increase linked to whisker stimulation could be observed in this brain area. If we hypothesize that lactate is produced by astrocytes during brain activity, and is further transferred to neurons, it may be surprising not to observe an accumulation of lactate in these KD rats, in which lactate cannot enter neurons. To better understand this apparent paradox, we decided to perform BOLD fMRI experiments to detect signs of local brain activation (using the BOLD signal as a surrogate marker for activation). While a positive BOLD signal was observed in 95% of Ctrl rats, the BOLD signal was lost in MCT2-KD rats (only a small signal

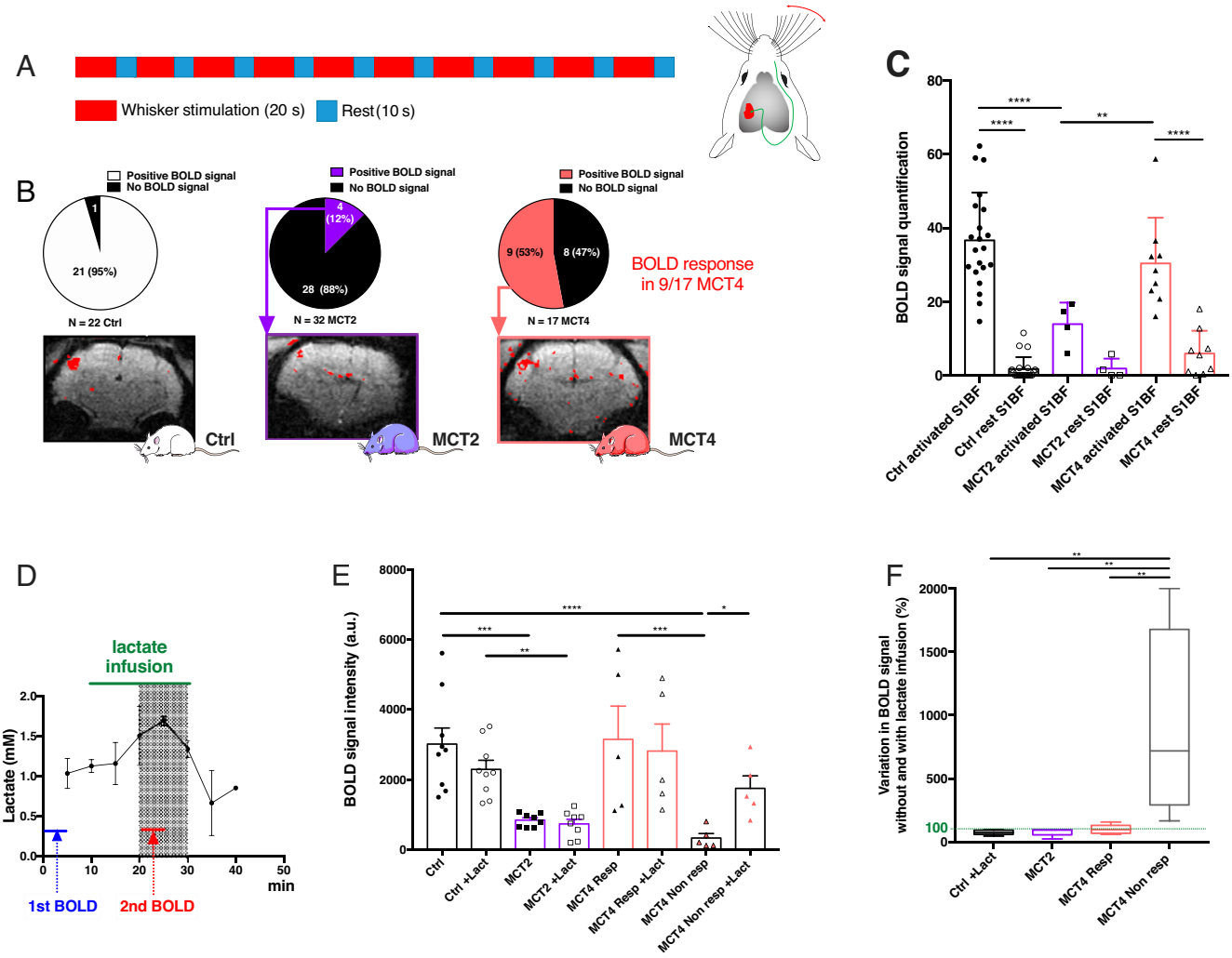

Fig. 3. Effect of cell-specific MCT2 or MCT4 down-regulation in the barrel cortex on the BOLD fMRI response during whisker stimulation and its putative rescue by lactate infusion. (*A*) Whisker stimulation paradigm (activation: 20 s, 8 Hz; rest: 10 s, during the entire fMRI acquisition: 600 scans, 5 min). (*B*) Distribution of positively/negatively responding animals and typical BOLD fMRI images for Ctrl (n = 22), MCT2-KD (n = 32), and MCT4-KD (n = 17) rats. (*C*) Quantification of BOLD fMRI signals (only for positively-responding animals). (*D*) Lactate concentration kinetics in the barrel cortex during peripheral lactate infusion. Lactate content was determined every 5 min by localized ^{1}H-NMR spectroscopy in the barrel cortex during lactate infusion (20 min) in the tail vein. The highest lactate concentration is reached in the shaded gray zone. Based on this kinetics, the best time window to acquire the second BOLD fMRI was selected (red line). n = 2. (*E*) Rescue experiments: BOLD fMRI was performed before (closed symbols) and 10 min after starting lactate infusion (open symbols) in Ctrl (n = 9, circles), MCT2-KD (n = 8, squares), and MCT4-KD (n = 10, triangles) rats. *P < 0.05; **P < 0.01; ***P < 0.001; ****P < 0.0001; ANOVA followed by a Fisher's LSD test. (*F*) Variation in BOLD signal intensity between acquisitions (shown in *E*) performed before and during lactate infusion (%, minimum to maximum and median). **P < 0.01; ANOVA followed by a Fisher's LSD test. The dashed green line represents no variation (100%).

was observed in 4 of 32 animals). These results confirm previous findings obtained using a lentiviral vector to express a similar shMCT2 sequence that prevented the BOLD response in the barrel cortex upon whisker stimulation (20). Based on these data, we can conclude that down-regulation of the neuronal lactate transporter leads to the suppression of the mechanism that is at the origin of the BOLD signal, and therefore to an impairment of the neurovascular coupling. Since no increase in lactate levels was measured in fMRS experiments, MCT2 down-regulation also leads to an apparent impairment of the neurometabolic coupling. Thus, it can be suggested that neuronal MCT2 down-regulation alters somehow the mechanisms leading to neurovascular and neurometabolic responses occurring after a stimulation within the barrel cortex.

Similarly to MCT2, down-regulation of the astroglial lactate transporter MCT4 in the rat barrel cortex prevented the lactate increase caused by whisker stimulation. In this regard, it seems that the neurometabolic coupling is impaired as well with astroglial MCT4 down-regulation, emphasizing the importance of an intact lactate shuttling between astrocytes and neurons for this process. Surprisingly, for the BOLD signal, results obtained with MCT4-KD rats represent a dichotomous situation between those for Ctrl rats and the ones for MCT2-KD rats. Indeed, the BOLD signal was present in about half of the animals but absent in the other half, which suggests that local brain activation (and the associated neurovascular coupling) was not systematically lost [efficiency of MCT4 down-regulation after stereotaxic injection in the S1BF was previously confirmed (27)]. This situation suggests the existence of a threshold-like effect. Unlike neurons, which only have the MCT2 isoform, astrocytes express both isoforms 1 and 4. Moreover, they express lactate channels that also allow lactate release in an activity-dependent manner (34) and participate in lactate shuttling in awake mice (35). We can then assume that for MCT4-KD rats, the presence of MCT1 transporters as well as lactate channels still allows some lactate release. This export would be

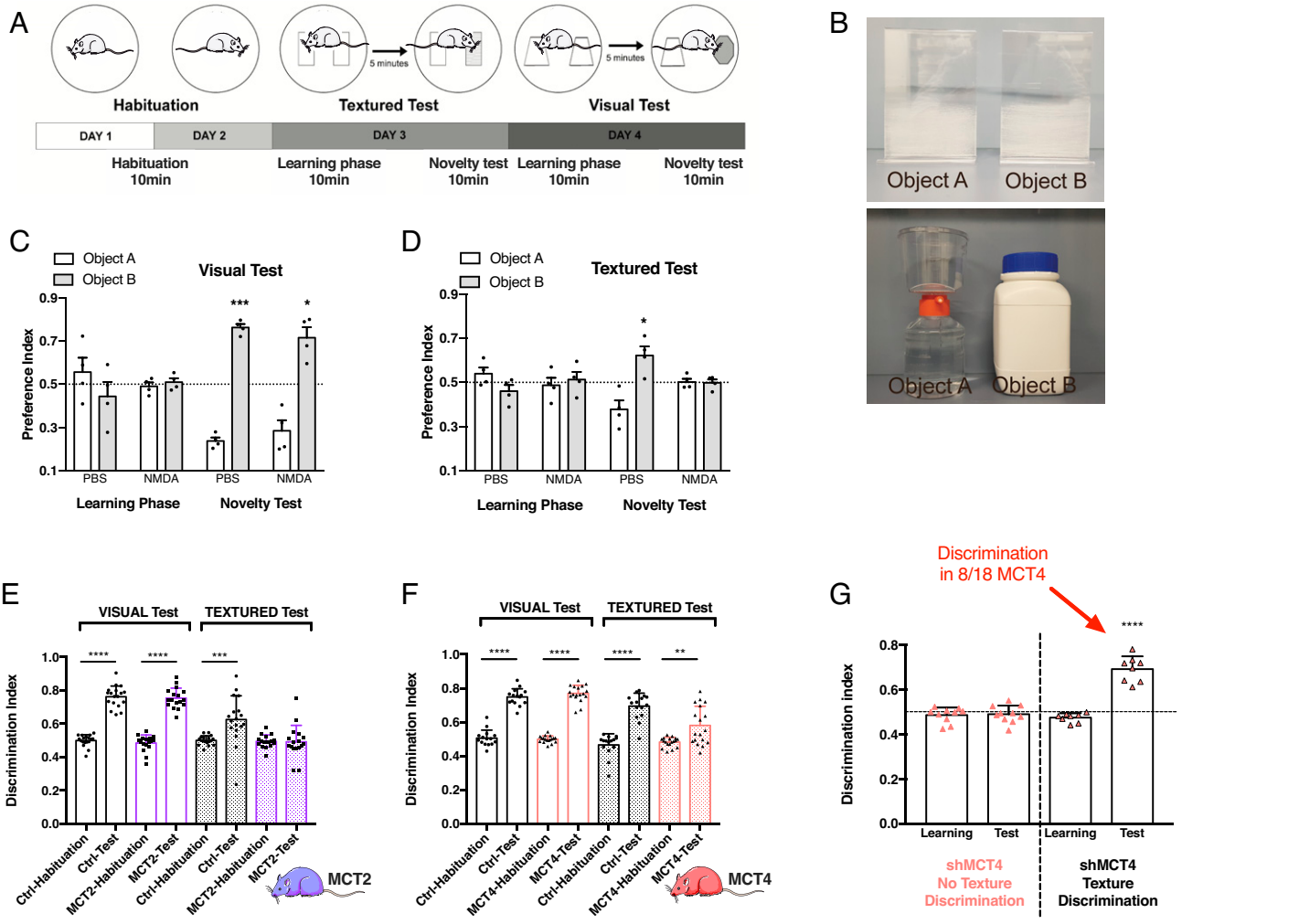

Fig. 4. Effect of cell-specific MCT2 or MCT4 down-regulation in the barrel cortex on performance in the visual and textured novel object recognition tasks. (*A*) Schematic representation of the protocol to perform both the textured and visual novel recognition tasks. The test is divided in 4 consecutive days. On days 1 and 2, animals were habituated to the arena for 10 min. On day 3, the animal was submitted to the textured task, composed of 10 min of learning, 5 min of rest, and 10 min of test with one of the objects that was exchanged. In the textured task, the novel object was identical in size, shape and color but different in term of texture (smooth versus rough). Finally, on day 4, the animal was submitted to the visual task. The difference with the third day was that the novel object was different in term of shape and color. For the 2 last days, the time spent exploring the objects was measured. (*B*) Pictures of the objects used for the textured and visual tasks. (*C*) Effect of an excitotoxic lesion in the barrel cortex on performance in the visual novel object recognition task; preference indexes for the visual task of animals injected with PBS (Phosphate buffered saline) or NMDA 1 M. The dashed line corresponds to chance level, when the animal equally explored the two objects. Data are presented as mean ± SEM $*P < 0.05$; $***P < 0.001$; ordinary one-way ANOVA, followed by Fisher's LSD test. $n = 6$ rats. (*D*) Effect of an excitotoxic lesion in the barrel cortex on performance in the tNOR; preference indexes for the textured task of animals injected with PBS or NMDA 1 M. The dashed line corresponds to chance level, when the animal equally explored the two objects. Data are presented as mean ± SEM $*P < 0.05$; ordinary one-way ANOVA, followed by Fisher's LSD test. $n = 6$. (*E*) Discrimination indexes for the vNOR and the tNOR for Ctrl and MCT2-KD animals. Data are presented as mean ± SEM $***P < 0.001$; $****P < 0.0001$; unpaired t test between habituation and test. Ctrl, $n = 18$; MCT2, $n = 16$. (*F*) Discrimination indexes for the vNOR and the tNOR for Ctrl and MCT4-KD animals. Data are presented as mean ± SEM $**P < 0.01$; $****P < 0.0001$; unpaired t test between habituation and test. Ctrl, $n = 15$; MCT4, $n = 18$. (*G*) Discrimination indexes for the learning and the test phases of the tNOR task for MCT4-KD animals, which was divided in two groups ($n = 18$). Orange triangles: MCT4-KD animals with no texture discrimination, $n = 10$; black and orange triangles: MCT4-KD animals with texture discrimination, $n = 8$. Data are presented as mean ± SEM $****P < 0.0001$. The horizontal black dashed line corresponds to an equal exploration of the two objects.

insufficient to measure by fMRS the same steady-state level as the one measured in Ctrl rats upon activation, but would be sufficient, at least in some rats, to maintain the appearance of the BOLD signal in the activated zone. Indeed, if enough lactate comes out of astrocytes, or is sufficiently present in the extracellular space, it can then be sensed by neurons (MCT2 is still present). If used extensively, such as during brain activation, then lactate cannot accumulate in the extracellular space and no increase can be measured during in vivo fMRS. According to this hypothesis, astrocytes would therefore supply under physiological conditions more lactate than is necessary for neurons, which is in accordance with the new steady-state level of lactate concentration that is measured. We may hypothesize that a lactate concentration threshold may exist to support brain activation, which was reached only in half of the MCT4-KD rats. This hypothesis would also fit with rescue experiments, in which lactate infusion was able to rescue the BOLD signal in nonresponding MCT4 animals.

Altogether, our data suggest that lactate supply to neurons by astrocytes could somehow regulate neuronal network activity and define a previously unrecorded threshold of excitability. This effect would be entirely prevented by neuronal MCT2

down-regulation but not systematically following astroglial MCT4 down-regulation, depending on the resulting lactate levels, which may fluctuate (according to the extent of astroglial MCT4 down-regulation). Indeed, evidence has been provided that lactate can act as a signal to modulate neuronal excitability (10). This action of lactate could be mediated via several described mechanisms, including an effect on NMDA receptors, on pH, on ATP-sensitive potassium channels, or on lactate receptors. It is purported that such an effect of lactate over a region corresponding to a barrel within the S1BF area would promote the capacity of the neuronal network within that structure to fine-tune in a coordinated manner neuronal processing and promote learning and memory processes.

The possibility that reducing neuronal MCT2 expression or astroglial MCT4 expression might also interfere with behavioral performance that relies on the activation of the barrel cortex was tested. MCT2 down-regulation led to an important deficit of S1BF function, reflected by the absence of discrimination between the objects during the tNOR task. However, those animals were still able to discriminate the objects during the vNOR task. Results obtained in astroglial MCT4 down-regulated animals reflected those obtained in BOLD fMRI experiments. About half of the animals were impaired in the tNOR task. These results show that the memory deficit seen in the tNOR task was caused by a specific deficit in the processing of somatosensory information in the barrel cortex, and not a global impairment in learning or a deficit related to the other brain structures involved in the task. These findings concur with several others, indicating that interfering with MCT expression on astrocytes and neurons, and lactate shuttling between the two cell types, alters learning and memory performances in a number of spatial and nonspatial tasks (36–41). While previous studies were targeting either the hippocampus or the striatum, our study demonstrates an effect on behavioral performance after modifying expression in a specific cortical area. This finding reinforces the view that lactate shuttling between astrocytes and neurons is a fundamental process present in various brain regions that is essential to sustain cognition.

In conclusion, our data indicate that lactate shuttling via MCTs between astrocytes and neurons is necessary to give rise to both neurovascular and neurometabolic couplings linked to brain activity. Since functional brain imaging relies on signals arising from these processes to map brain activity, our findings emphasize the key contribution of astrocytes to brain imaging. Finally, as lactate shuttling was found here to be a limiting factor to sustain cognitive function subserved by local cortical activation, it becomes of interest to consider the role of this astrocyte-dependent mechanism in the context of neurodegenerative diseases. Indeed, as cortical hypometabolism is a classic observation in these pathologies and has been evidenced even at asymptomatic stages, astrocytes and their regulation of energy metabolism might constitute a novel preventive therapeutic target.

Materials and Methods

Animals. All animal procedures were conducted in accordance with the Animal Experimentation Guidelines of the European Communities Council Directive of November 24, 1986 (86/609/EEC). Protocols met the ethical guidelines of the French Ministry of Agriculture and Forests, and were approved by the local ethics committees (Comité d'éthique pour l'expérimentation Animale Bordeaux 50112090-A and the Swiss "Service de la Consommation et des Affaires Vétérinaires, SCAV, authorization 3101.1). Male Wistar RJ-HAN (Janvier Laboratories) were kept on a 12:12-h light:dark cycle with food and water ad libitum.

AAV2/DJ-Based Viral Vector Generation. AAV2/DJ-based viral vectors were prepared exactly as described in detail in Jollé et al. (27). Briefly, four constructs were made to target alternatively neurons or astrocytes. For neuron-specific expression, an shRNA sequence targeting MCT2 (shMCT2; TAGGATTAATAGCCAACACTA) or a control noncoding sequence (shUNIV2; TGTATCGATCACGAGACTAGC) embedded in a miR30E sequence was positioned after a mCherry sequence under the control of a CBA (Chicken-β-actin) promoter. For astrocyte-specific expression, an shRNA sequence targeting MCT4 (shMCT4; GGTGAGCTATGCTAAGGATAT) or a control noncoding sequence (shUNIV4; TGTATCGATCACGAGACTAGC) embedded in a miR30E sequence was positioned after a mCherry sequence under the control of a G1B3 (a glial fibrillary acidic protein-derived) promoter (42). Each construct was incorporated in an AAV2/DJ serotype to obtain four distinct AVV2/DJ-based viral vectors. All these viral vectors have been tested previously for their specificity and efficacy in the rat barrel cortex (27). Since no difference was observed between animals injected with either AAV2/DJ-CBA-shUNIV2 or AAV2/DJ-G1B3-shUNIV4, data from these animals were pooled and considered as Ctrl data.

Stereotaxic Injection. Surgeries were performed on 7-wk-old animals. Animals were anesthetized with isoflurane (5% for the induction and 3% to maintain the anesthesia). AAVs or PBS were injected in both hemispheres (S1BF: anteroposterior = −2,3 mm; mediolateral = ±5 mm; dorsoventral = −3 mm). Viral vectors were injected with 34-G steel cannula fixed on a cannula holder and linked to a 10-μL Hamilton syringe and an infusion pump. For each site, 4 μL of viral vector were injected at 0.2 μL/min. Cannulas were left in the brain for 5 min after the injection, and then slowly removed. Skin was closed using 4.0 sterile suture thread. Sterile NaCl 0.9% solution (1 mL) was delivered to the rat by intraperitoneal injection to avoid dehydration after surgery, and healing cream was applied on the head. Sugar-taste Paracetamol was delivered to the animal in water (1 g per cage for rats) for 72 h. Animals were monitored until complete awakening, and every day for 3 d after the surgery. All viral vectors were injected at a final concentration of 1×10^8 vg per site.

In Vivo Functional ^{1}H-MRS and BOLD fMRI. Experiments were conducted on a 7T Bruker BioSpec system (70/20) equipped with a 20-cm horizontal bore, a gradient system capable of 660-mT/m maximum strength, and 110-μs rise time. A surface coil (10-mm inner diameter; Bruker) was used for excitation and signal reception. Rats were anesthetized using medetomidine hydrochloride (Domitor, Vetoquinol SA; 1 mg/mL, 240 μg/kg/h – perfusion rate: 20 μL/min). Whisker activation was performed directly into the magnet using an air-puff system (32). For this purpose, right whiskers were taped such as a sail was made and this sail was blown at 8 Hz during the acquisition time (activation paradigm: 20 s activation – 10 s rest, duration 5 min 20 s for fMRS and 5 min for fMRI). In order to place correctly the voxel in the S1BF area, a T_2-weighted sequence was performed (RARE sequence): 16 slices, 1-mm thick, field-of-view 5 × 5 cm. A voxel was then located in the S1BF area (2 × 2.5 × 3 mm) and in vivo spectroscopy was performed either at rest or during whisker activation using a LASER sequence (TE 20 ms, TR 2.500 ms, 128 scans). Spectra were analyzed and lactate was quantified using LCModel (Provencher) software using water-scaling (WCONC 43300).

Finally, functional imaging was performed. The BOLD response was measured (using the activation paradigm) in four slices of 0.7-mm thickness using a single short gradient echo, echo planar imaging sequence (TR = 500 ms, TE = 16.096 ms, field-of-view 25 × 25 mm^2, matrix size 96 × 96 and bandwidth of 33,333 Hz). Images were reconstructed and analyzed using FUN TOOL fMRI processing (Bruker software).

Rescue Experiments. Rats were anesthetized using medetomidine hydrochloride (Domitor, Vetoquinol SA; 1 mg/mL, 240 μg/kg/h – perfusion rate: 20 μL/min) as previously, using an amagnetic tail vein catheter. A three-way stopcock was used for lactate infusion [sodium salt, 534 mM, with a flow rate monitored from 15 mL/h to 1.23 mL/h during the first 25 min (1)]. Measurement of the BOLD response was performed twice. The first acquisition was performed during whisker activation, without lactate infusion. Then, lactate infusion was initiated and, 10 min later, the second BOLD experiment was started. Lactate concentration was the highest in the barrel cortex in this time window, as previously determined by in vivo ^{1}H-MRS performed every 5 min in the barrel cortex during the lactate infusion protocol period (25 min).

Ex Vivo MRS.

Whisker activation on awake animals. Experiments were performed in awake animals 6 wk after AAV injections. Animals were slightly held on a Plexiglas support during the stimulation. Before infusion experiments, each animal was accustomed to the experimental set up (at least three times, 1 h) to avoid any stress and ^{13}C-infusion experiments were performed once rats demonstrated that they lie quietly. Right whiskers were mechanically stimulated at a rate of 8 Hz for 1 h. To stimulate the maximum of whiskers, they were cut to an equivalent length: 2.5 cm. Infusions were performed in the tail vein during 1 h (to reach the isotopic steady state), during whisker stimulation. Rats

were infused with a solution containing [1-^{13}C glucose] (750 mM, Cambridge isotope, 99% enrichment) + lactate (sodium salt, 534 mM). Intravenous infusions were carried out using a syringe pump that allows a flow such as glucose and lactate concentrations in the blood remain constant (the infusate flow was monitored to obtain a time-decreasing exponential from 15 mL/h to 1.23 mL/h during the first 25 min after which the rate was kept unchanged). At the end of the experiment, a sample of blood was removed; rats were rapidly killed by cerebral-focused microwaves (5 KW, 1 s, Sacron8000, Sairem), the only way to immediately stop all enzymatic activities and to avoid postmortem artifacts such as anaerobic lactate production, as already demonstrated in Sampol et al. (33).

S1BF areas (right: nonactivated and left: activated) were removed, using a rat brain matrix that allows precise and reproducible dissection of the selected brain regions, dipped in liquid nitrogen, and kept at −80 °C until NMR analyses, conducted on a Bruker DPX500 spectrometer equipped with a HR-MAS (high resolution at the magic angle spinning) probe after perchloric acid extracts. Indeed, HR-MAS allows performing spectra with high spectral resolution not only directly on biopsies but also on small perchloric acid extract volumes (50 μL).

Perchloric acid extracts. A volume of 200 μL of 0.9 M perchloric acid was added to the frozen S1BF biopsies (around 30 mg) and further sonicated (at 4 °C). The mixture was then centrifuged at 5,000 × *g* for 15 min (4 °C). The brain extract was neutralized with KOH to pH = 7.2, and centrifuged again to eliminate potassium perchlorate salts. Supernatant was lyophilized, the final powder was dissolved in 100 μL D_2O and bivalent cations were eliminated using Chelex 100 resin beads. Ethylene glycol was added and used as an external reference (1 M, peak at 63 ppm, 2 μL).

POCE sequence. This sequence was used to determine the ^{13}C-specific enrichment (SE) at selected metabolite carbon positions using the (^{13}C-^{1}H) heteronuclear multiquanta correlation (43, 44). Briefly, two spectra are acquired: the first scan corresponds to a standard spin-echo experiment without any ^{13}C excitation and a second scan involves a ^{13}C-inversion pulse to get coherence transfer between coupled ^{13}C and ^{1}H nuclei. Subtraction of two alternate scans leads to the editing of ^{1}H spins coupled to ^{13}C spins (scalar coupling constant JCH = 127 Hz). ^{13}C-decoupling was applied during the acquisition to collapse the ^{1}H-^{13}C coupling under a single 1H resonance. Flip angles for rectangular pulses were carefully calibrated on both radiofrequency channels before each experiment. The relaxation delay was 8 s for a complete longitudinal relaxation. The ^{13}C-SE was calculated as the ratio of the area of a given resonance on the edited ^{13}C-^{1}H spectrum to its area on the standard spin-echo spectrum. The reproducibility and accuracy of the method were previously assessed using several mixtures of ^{13}C-labeled amino acids and lactate with known fractional enrichments and both were better than 5%.

Behavioral Studies. Animals were given 3 wk to recover from surgery (AAV injections). They were habituated to the housing of the behavioral area for 2 wk. During the first 2 d of behavioral testing, rats were habituated for 10 min to the circular open field arena (45 × 10 cm, light gray). The floor and walls were cleaned with ethanol 70% to avoid scent trails guiding the animals between test sessions. On the third day, the tNOR was performed. For the first step, the animal was released on one side of the arena, facing the wall, at equal distance from the two identical objects. The objects were placed equidistant from the center of the arena and from the walls. Each rat was allowed to explore the objects for 10 min. The animal was then removed from the arena for 5 min. During this retention period, the arena and the objects were wiped with ethanol 70%. One of the familiar objects was replaced by the novel object. This object was visually identical to the familiar object (in size, shape, color) but exhibited a different texture (smooth or rough). To avoid any texture discrimination coming from forepaws and to test only whisker sensitivity, only the lower part of the object had a different texture. Then for the second step, the rat was returned into the test arena and allowed to explore the objects for 10 min. The time each rat spent physically exploring the objects was recorded during both steps.

On the fourth day, the vNOR took place. The rat was allowed to explore the two identical objects for 10 min. Then the rat was removed from the arena for 5 min. The arena and objects were wiped with ethanol 70%. One object was replaced by a novel object. This object was visually different from the familiar one. Then the animal was reintroduced into the arena and allowed to explore the objects for 10 min.

In the visual task, object A was 10 cm in diameter × 22 cm in height and object B was 10 × 10 × 20 cm. In the textured task, the two objects were 10.5 × 5 × 15.5 cm. Object A was rough and Object B was smooth.

The novelty preference index was calculated as $Preference\ Index = \frac{Time_{Object\ A/B}}{(Time_{Object\ A} + Time_{Object\ B})}$. Animals that did not explore the two objects for at least 4 s were excluded from the analysis. The visual (vNOR) and the textured (tNOR) tasks were recorded using Media Recorder v.4.0.2. The time of exploration was blindly and manually scored using Kinoscope v0.3.0.

Statistical Analysis. Results are presented as mean ± SEM. Statistical analyses were performed with GraphPad Prism (v7.04). For behavioral analyses, a Wilcoxon's test was applied to compare the novelty preference index to 0.5 (chance value). For BOLD fMRI and fMRS, data were analyzed using ordinary one-way ANOVA followed by a Fisher's least-significant difference (LSD) test or paired-*t* test. Results were considered significant when $P < 0.05$.

Data Availability. All study data are included in the main text.

ACKNOWLEDGMENTS. A.-K.B.-S. and L.P. have received financial support from an international French (ANR)/Swiss (FNS) Grants ANR-15-CE37-0012 and FNS 310030E-164271. L.P. also received financial support for this project from the program IdEx Bordeaux ANR-10-IDEX-03-02. A.-K.B.-S. has also received financial support from the French State in the context of the "Investments for the future" Programme IdEx and the LabEx TRAIL, reference ANR-10-IDEX and ANR-10-LABX-57, which also supported H.R. N.D. has received support from the BIOS and Panacée Foundations. I.B. is supported by the LabCom I3M, Common Laboratory CNRS-Siemens, University of Poitiers and Poitiers University Hospital and by Region Nouvelle Aquitaine. E.R.Z. is supported by Conselho Nacional de Pesquisas (CNPq) 435642/2018-9 and 312410/2018-2, Instituto Serrapilheira Serra-1912-31365, Brazilian National Institute of Science and Technology in Excitotoxicity and Neuroprotection 465671/2014-4, Fundação de Amparo à Pesquisa do Estado do Rio Grande do Sul (FAPERGS)/MS/CNPq/Secretaria da Saúde do Rio Grande do Sul–Programa Pesquisa para a Sus 30786.434.24734.23112017, ARD/FAPERGS 54392.632.30451.05032021, and Alzheimer's Association AARGD-21-850670.

1. A. K. Bouzier *et al.*, The metabolism of [3-(13)C]lactate in the rat brain is specific of a pyruvate carboxylase-deprived compartment. *J. Neurochem.* **75**, 480–486 (2000).
2. D. Smith *et al.*, Lactate: A preferred fuel for human brain metabolism in vivo. *J. Cereb. Blood Flow Metab.* **23**, 658–664 (2003).
3. G. van Hall *et al.*, Blood lactate is an important energy source for the human brain. *J. Cereb. Blood Flow Metab.* **29**, 1121–1129 (2009).
4. F. Boumezbeur *et al.*, The contribution of blood lactate to brain energy metabolism in humans measured by dynamic 13C nuclear magnetic resonance spectroscopy. *J. Neurosci.* **30**, 13983–13991 (2010).
5. L. Pellerin, P. J. Magistretti, Glutamate uptake into astrocytes stimulates aerobic glycolysis: A mechanism coupling neuronal activity to glucose utilization. *Proc. Natl. Acad. Sci. U.S.A.* **91**, 10625–10629 (1994).
6. A. K. Bouzier-Sore *et al.*, Competition between glucose and lactate as oxidative energy substrates in both neurons and astrocytes: A comparative NMR study. *Eur. J. Neurosci.* **24**, 1687–1694 (2006).
7. A. K. Bouzier-Sore, P. Voisin, P. Canioni, P. J. Magistretti, L. Pellerin, Lactate is a preferential oxidative energy substrate over glucose for neurons in culture. *J. Cereb. Blood Flow Metab.* **23**, 1298–1306 (2003).
8. L. Pellerin, P. J. Magistretti, Sweet sixteen for ANLS. *J. Cereb. Blood Flow Metab.* **32**, 1152–1166 (2012).
9. L. F. Barros, B. Weber, CrossTalk proposal: An important astrocyte-to-neuron lactate shuttle couples neuronal activity to glucose utilisation in the brain. *J. Physiol.* **596**, 347–350 (2018).
10. P. J. Magistretti, I. Allaman, Lactate in the brain: From metabolic end-product to signalling molecule. *Nat. Rev. Neurosci.* **19**, 235–249 (2018).
11. G. Bonvento, J. P. Bolaños, Astrocyte-neuron metabolic cooperation shapes brain activity. *Cell Metab.* **33**, 1546–1564 (2021).
12. A. Volkenhoff *et al.*, Glial glycolysis is essential for neuronal survival in *Drosophila*. *Cell Metab.* **22**, 437–447 (2015).
13. L. Liu, K. R. MacKenzie, N. Putluri, M. Maletić-Savatić, H. J. Bellen, The glia-neuron lactate shuttle and elevated ROS promote lipid synthesis in neurons and lipid droplet accumulation in glia via APOE/D. *Cell Metab.* **26**, 719–737.e6 (2017).
14. F. Baeza-Lehnert *et al.*, Non-canonical control of neuronal energy status by the Na^+ pump. *Cell Metab.* **29**, 668–680.e4 (2019).
15. C. M. Díaz-García *et al.*, Neuronal stimulation triggers neuronal glycolysis and not lactate uptake. *Cell Metab.* **26**, 361–374.e4 (2017).
16. J. J. Laschet *et al.*, Glyceraldehyde-3-phosphate dehydrogenase is a $GABA_A$ receptor kinase linking glycolysis to neuronal inhibition. *J. Neurosci.* **24**, 7614–7622 (2004).
17. A. Herrero-Mendez *et al.*, The bioenergetic and antioxidant status of neurons is controlled by continuous degradation of a key glycolytic enzyme by APC/C-Cdh1. *Nat. Cell Biol.* **11**, 747–752 (2009).
18. L. K. Fellows, M. G. Boutelle, M. Fillenz, Physiological stimulation increases nonoxidative glucose metabolism in the brain of the freely moving rat. *J. Neurochem.* **60**, 1258–1263 (1993).
19. Y. Hu, G. S. Wilson, A temporary local energy pool coupled to neuronal activity: Fluctuations of extracellular lactate levels in rat brain monitored with rapid-response enzyme-based sensor. *J. Neurochem.* **69**, 1484–1490 (1997).

20. L. Mazuel *et al.*, A neuronal MCT2 knockdown in the rat somatosensory cortex reduces both the NMR lactate signal and the BOLD response during whisker stimulation. *PLoS One* **12**, e0174990 (2017).
21. J. Prichard *et al.*, Lactate rise detected by 1H NMR in human visual cortex during physiologic stimulation. *Proc. Natl. Acad. Sci. U.S.A.* **88**, 5829–5831 (1991).
22. D. Sappey-Marinier *et al.*, Effect of photic stimulation on human visual cortex lactate and phosphates using 1H and 31P magnetic resonance spectroscopy. *J. Cereb. Blood Flow Metab.* **12**, 584–592 (1992).
23. K. Pierre, L. Pellerin, Monocarboxylate transporters in the central nervous system: Distribution, regulation and function. *J. Neurochem.* **94**, 1–14 (2005).
24. K. Pierre, P. J. Magistretti, L. Pellerin, MCT2 is a major neuronal monocarboxylate transporter in the adult mouse brain. *J. Cereb. Blood Flow Metab.* **22**, 586–595 (2002).
25. K. Rosafio, X. Castillo, L. Hirt, L. Pellerin, Cell-specific modulation of monocarboxylate transporter expression contributes to the metabolic reprograming taking place following cerebral ischemia. *Neuroscience* **317**, 108–120 (2016).
26. O. Chiry *et al.*, Expression of the monocarboxylate transporter MCT1 in the adult human brain cortex. *Brain Res.* **1070**, 65–70 (2006).
27. C. Jollé, N. Déglon, C. Pythoud, A. K. Bouzier-Sore, L. Pellerin, Development of efficient AAV2/DJ-based viral vectors to selectively downregulate the expression of neuronal or astrocytic target proteins in the rat central nervous system. *Front. Mol. Neurosci.* **12**, 201 (2019).
28. A. K. Bouzier, B. Quesson, H. Valeins, P. Canioni, M. Merle, [1-(13)C]glucose metabolism in the tumoral and nontumoral cerebral tissue of a glioma-bearing rat. *J. Neurochem.* **72**, 2445–2455 (1999).
29. V. Briz *et al.*, The non-coding RNA BC1 regulates experience-dependent structural plasticity and learning. *Nat. Commun.* **8**, 293 (2017).
30. H. P. Wu, J. C. Ioffe, M. M. Iverson, J. M. Boon, R. H. Dyck, Novel, whisker-dependent texture discrimination task for mice. *Behav. Brain Res.* **237**, 238–242 (2013).
31. E. D. Kirby, K. Jensen, K. A. Goosens, D. Kaufer, Stereotaxic surgery for excitotoxic lesion of specific brain areas in the adult rat. *J. Vis. Exp.* **65**, e4079 (2012).
32. J. Blanc *et al.*, Functional magnetic resonance spectroscopy at 7 T in the rat barrel cortex during whisker activation. *J. Vis. Exp.* **144**, e58912 (2019).
33. D. Sampol *et al.*, Glucose and lactate metabolism in the awake and stimulated rat: A (13)C-NMR study. *Front. Neuroenergetics* **5**, 5 (2013).
34. T. Sotelo-Hitschfeld *et al.*, Channel-mediated lactate release by K^+-stimulated astrocytes. *J. Neurosci.* **35**, 4168–4178 (2015).
35. M. Zuend *et al.*, Arousal-induced cortical activity triggers lactate release from astrocytes. *Nat. Metab.* **2**, 179–191 (2020).
36. G. Descalzi, V. Gao, M. Q. Steinman, A. Suzuki, C. M. Alberini, Lactate from astrocytes fuels learning-induced mRNA translation in excitatory and inhibitory neurons. *Commun. Biol.* **2**, 247 (2019).
37. D. L. Korol, R. S. Gardner, T. Tunur, P. E. Gold, Involvement of lactate transport in two object recognition tasks that require either the hippocampus or striatum. *Behav. Neurosci.* **133**, 176–187 (2019).
38. C. Netzahualcoyotzi, L. Pellerin, Neuronal and astroglial monocarboxylate transporters play key but distinct roles in hippocampus-dependent learning and memory formation. *Prog. Neurobiol.* **194**, 101888 (2020).
39. M. Tadi, I. Allaman, S. Lengacher, G. Grenningloh, P. J. Magistretti, Learning-induced gene expression in the hippocampus reveals a role of neuron-astrocyte metabolic coupling in long term memory. *PLoS One* **10**, e0141568 (2015).
40. L. A. Newman, D. L. Korol, P. E. Gold, Lactate produced by glycogenolysis in astrocytes regulates memory processing. *PLoS One* **6**, e28427 (2011).
41. A. Suzuki *et al.*, Astrocyte-neuron lactate transport is required for long-term memory formation. *Cell* **144**, 810–823 (2011).
42. M. Humbel *et al.*, Maximizing lentiviral vector gene transfer in the CNS. *Gene Ther.* **28**, 75–88 (2021).
43. R. Freeman, T. H. Mareci, G. A. Morris, Weak satellite signals in high-resolution NMR spectra: Separating the wheat from the chaff. *J. Magn. Reson.* **42**, 341–345 (1981).
44. D. L. Rothman *et al.*, 1H-Observe/13C-decouple spectroscopic measurements of lactate and glutamate in the rat brain in vivo. *Proc. Natl. Acad. Sci. U.S.A.* **82**, 1633–1637 (1985).